Microwave Irradiated and Thermally Heated Olive Stone Activated Carbon for Nickel Adsorption from Synthetic Wastewater: A Comparative Study

Tamer M. Alslaibi and Ismail Abustan
School of Civil Engineering, Engineering Campus, Universiti Sains Malaysia, 14300 Nibong Tebal, Pulau Pinang, Malaysia

Mohd Azmier Ahmad
School of Chemical Engineering, Engineering Campus, Universiti Sains Malaysia, 14300 Nibong Tebal, Pulau Pinang, Malaysia

Ahmad Abu Foul
Environmental Engineering, Islamic University of Gaza, Palestine

DOI 10.1002/aic.14236
Published online October 8, 2013 in Wiley Online Library (wileyonlinelibrary.com)

In attempt to compare the removal efficiency and yield of the activated carbon prepared using the conventional and microwave-assisted heating is the focus of this work. Toward this olive stone (a biomass precursor) is activated using the popular activating agent potassium hydroxide. The process optimization exercise is carried out by using the standard full factorial statistical design of experiments (response surface methodology). The activated carbons prepared under the optimized conditions are compared based on the adsorption capacity and yield. The adsorption capacity was found higher using microwave heating as compared with conventional heating. The microwave heating requires significantly lesser holding time as compared to conventional heating method to produce activated carbon of comparable quality, with higher yield. The BET surface area of carbon using microwave heating is significantly higher than the conventional heating. Although the mesopore surface area of carbon is not vary significantly, the activation time, power, and nitrogen gas consumption are significantly lower than the conventional heating rendering that the activation process via microwave is more economical than that via conventional heating. The adsorption isotherm data fitted the Langmuir isotherm well and the monolayer adsorption capacity was found to be 12.0 and 8.42 mg/g for microwave and thermally heated activated carbon, respectively. Regeneration studies showed that microwave-irradiated and thermally heated olive stone could be used several times by desorption with an HCl reagent. Both carbons can be used for the efficient removal of Ni^{2+} (>99%) from contaminated wastewater. © 2013 American Institute of Chemical Engineers *AIChE J*, 60: 237–250, 2014

Keywords: activated carbon, nickel adsorption, microwave and thermal heating, olive stone, response surface methodology

Introduction

Heavy metals appear in wastewater discharged from hospitals[1] and various industries, including smelting, metal plating, Cd-Ni batteries, and alloy manufacturing.[2] In the field of water pollution, toxic metal removal from wastewater is a matter of great interest because such metals cause serious environmental degradation.[3] Heavy metals present ecological and human health issues because they do not undergo biological degradation, unlike certain organic pollutants.[4] Headache, dermatitis, dizziness, dry cough, nausea, vomiting, and cyanosis leading to capillary, hepatic, and renal damage, nervous disabilities, chest pain, cancer in lungs, nose, and bones are among the major human health issues caused by long-term Ni^{2+} exposure; thus, this toxic metal must be removed from wastewater to protect humans and the environment.[5] Due to the toxicity of the metal, the World Health Organization has set the international standard for Ni^{2+} discharged into surface waters at 0.02 mg/L.

The thermal heating method is usually adopted for the preparation of activated carbon; in this method, energy is produced by an electrical furnace. The method requires high energy consumption and long processing times, thereby prompting researchers to study the preparation of activated carbon using microwave technology.[6] During microwave heating, a tremendous thermal gradient from the interior of the char particle to its cool surface allows the microwave-induced reaction to proceed quickly and effectively at a low bulk temperature; energy savings and a shortened processing

Correspondence concerning this article should be addressed to I. Abustan at ceismail@eng.usm.my.

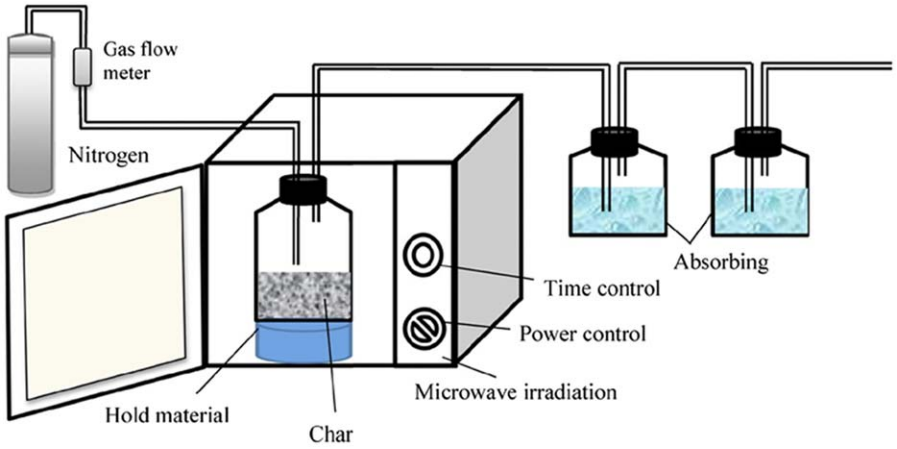

Figure 1. Schematic diagram of the preparation of activated carbon from OSs with KOH activation by microwave irradiation.

[Color figure can be viewed in the online issue, which is available at wileyonlinelibrary.com.]

time are the key advantages of microwave heating.[7] Microwave heating technology was recently applied to fabricate activated carbon for dye removal using agriculture by-products such as bamboo waste,[8,9] waste tea,[10] rice husk,[11] oil palm fiber,[12] pistachio nut shells,[13] cotton stalk,[14] date stones,[15] and mangosteen peel,[16] However, no studies on heavy metal removal using activated carbon prepared by microwave technology have been done yet.[17,18] Furthermore, the use of olive stone (OS) for activated carbon preparation via microwave technology has not been reported and studies concerning the optimization of activated carbon preparation conditions for Ni^{2+} removal using response surface methodology (RSM) are limited. The optimization of RSM is particularly useful when all of the independent variables and their levels and responses are not clearly known.[19] A standard RSM technique called a central composite design (CCD) is suitable for creating a quadratic surface and can help analyze interactions between parameters and optimize the effective parameters within a small number of experiments.[20]

The main objectives of this study include the following:

1. To investigate the efficiency of microwave-irradiated OS (MIOS) for removing Ni^{2+} from synthetic wastewater and compared to thermally heated OS (THOS) activated carbon.
2. To build equations of Ni^{2+} removal efficiency from synthetic wastewater and carbon yield with respect to MIOS and THOS preparation conditions.
3. To compare the optimized MIOS and THOS activated carbon in terms of the preparation conditions, characteristics, materials consumption, and adsorption capacities.

Material and Methods

Aqueous solution

A stock solution of Ni^{2+} was prepared by dissolving an appropriate amount of $NiCl_2.6H_2O$ (s) in deionized water. The stock solution was diluted with deionized water to obtain the desired concentration of 20 mg/L.

Preparation of activated carbon

OS waste was obtained from Gaza, Palestine. The OS waste was rinsed thrice with hot water and thrice with cold water and then dried in an oven at 105°C for 24 h to remove moisture. The samples were ground and sieved to a particle size of 2.0–4.75 mm.[21] Carbonization was carried out by loading 500 g of dried precursor into a stainless steel vertical tube reactor placed in a tube furnace at 600°C for 1 h under purified nitrogen (99.99%) flow. Potassium hydroxide (KOH) was used to activate the char via the chemical activation method. The amount of KOH used was adjusted to yield a certain impregnation ratio 0.5, 1.25, and 2, as calculated using Eq. (1):

$$\text{Impregnation ratio (IR)} = \frac{\text{dry weight of KOH pellets}}{\text{dry weight of char}} \quad (1)$$

Deionized water was then added to the KOH to dissolve all of the pellets. Impregnation was performed for 24 h at room temperature, thereby incorporating all of the chemicals into the core of the particles. After impregnation, the solution was filtered to obtain the residual char. First activation of impregnated char was carried out using a modified commercial microwave furnace with a frequency of 2.45 GHz at different power level ranging from 264 to 616 W and various radiation time ranging from 4 to 8 min under a nitrogen flow of 300 cm^3/min, as shown in Figure 1. For comparison, activated carbons were also prepared by conventional thermal method in an electrical furnace at different temperature level ranging from 400 to 800°C and various times ranging from 1 to 3 h under a nitrogen flow of 150 cm^3/min. The chosen conditions of nitrogen flow rates in microwave and conventional thermal methods are common in activation process.[12,13] The samples were then cooled to room temperature under nitrogen flow and washed with hot deionized water and 0.1 M HCl until the pH of the washed solution ranged from 6.5 to 7.

Design of experimental using RSM

RSM is a collection of mathematical and statistical techniques useful for modeling and analysis of problems in which a response of interest is influenced by several factors. In this study, RSM was used to assess the relationship between two responses (Ni^{2+} removal and carbon yield, %) and independent factors, as well as optimize the relevant conditions of factors to predict the optimal value of responses. Among other designs under RSM, CCD was used to study the

Table 1. Independent Factors and Their Coded Levels for CCD

Activation Method	factors	Code	Units	Coded Variable Levels −1	0	1
Microwave	Radiation power	X_1	(watt)	264	440	616
	Radiation time	X_2	(min)	4	6	8
	Impregnation ratio	X_3	–	0.5	1.25	2
Thermal	Temperature	X_1	(°C)	400	600	800
	Time	X_2	(h)	1	2	3
	Impregnation ratio	X_3	–	0.5	1.25	2

individual and synergetic effects of the three factors toward the responses.[10] CCD is suitable for fitting a quadratic surface and helps optimize the effective parameters with a minimum number of experiments and analyze the interaction between parameters.[8] The factors considered for MIOS included radiation power (X_1), radiation time (X_2), and chemical impregnation ratio (X_3). Meanwhile, the factors considered for THOS included temperature (X_1), time (X_2), and chemical impregnation ratio (X_3). These factors and their respective ranges were chosen based on the literature and our preliminary studies. The ranges and the levels of the factors investigated are given in Table 1.

The performance of the process was evaluated by analyzing Ni^{2+} removal efficiency and carbon yield by two methods. Each independent variable varied over three levels between −1 and +1 at the determined ranges based on several preliminary experiments. The total number of experiments obtained for the three factors was 20 ($=2^k+2k+6$), where k is the number of factors ($k=3$) as shown in Table 2. Fourteen experiments were enhanced with six replications to assess the pure error. As each factor only had three levels, the appropriate model is the quadratic model, expressed as Eq. (2)

$$Y=b_o+\sum_{i=1}^{k} b_i x_i+\sum_{i=1}^{k} b_{ii}x_i^2+\sum_{i=1}^{k-1}\sum_{j=i+1}^{k} b_{ij}x_i x_j+e_i \qquad (2)$$

where Y is the predicted response, b_0 is the constant coefficient, b_i is the linear coefficient, b_{ij} is the interaction coefficient, b_{ii} is the quadratic coefficient, and X_i and X_j are the coded values of the activated carbon preparation variables.

The qualities of the fit of polynomial models were expressed by the correlation coefficient (R^2). The model F-value (Fisher variation ratio), probability value (Prob > F), and adequate precision (AP) are the main indicators demonstrating the significance and adequacy of the used model.[22]

Activated carbon yield

The yield values of the MIOS and THOS were calculated based on the following equation:

$$\text{Yield } (\%)=\frac{\text{dry weight (g) of final activated carbon}}{\text{dry weight (g) of char}}\times 100 \qquad (3)$$

Analytical methods

Batch adsorption was performed in 20 flasks of 250-mL Erlenmeyer flasks. In each flask, we placed 100 mL of the synthetic wastewater with an initial Ni^{2+} concentration of 20 mg/L. Each of the prepared activated carbon samples 0.3 g was added to individual flasks as optimum dosage based on our preliminary experiments, which were then kept in an isothermal shaker at pH 5, 200 rpm, and 30°C until equilibrium was reached. After agitation, the solid was removed by filtration through a 0.45-μm pore size Whatman membrane filter paper. The final metal concentrations in the filtrates and in the initial solution were determined using an inductively coupled plasma optical emission spectroscopy system (Varian, 715-ES). The sorbed metal concentrations were obtained from the difference between the initial and final metal concentrations in solution. The percentage removal at equilibrium was calculated as follows:

$$\text{Removal } (\%)=\frac{C_0-C_e}{C_0}\times 100 \qquad (4)$$

Table 2. Experimental Factors and Responses

		MIOS					THOS				
		Factors			Responses		Factors			Responses	
Run no.	Type	X_1: power (W)	X_2: time (min)	X_3: IR	Ni removal Y_1 (%)	Yield Y_2 (%)	X_1: temp. (°C)	X_2: time (h)	X_3: IR	Ni removal Y_1 (%)	Yield Y_2 (%)
1	Center	440	6	1.25	88.00	88.14	600	2	1.25	99.06	79.10
2	Center	440	6	1.25	88.15	87.56	600	2	1.25	98.54	78.13
3	Center	440	6	1.25	87.91	88.78	600	2	1.25	98.48	78.53
4	Center	440	6	1.25	89.39	88.88	600	2	1.25	99.06	79.03
5	Center	440	6	1.25	88.62	87.86	600	2	1.25	98.92	77.81
6	Center	440	6	1.25	87.78	88.94	600	2	1.25	99.43	78.81
7	Axial	440	6	2.00	91.99	88.26	400	2	2.00	83.76	87.30
8	Axial	440	4	1.25	57.50	89.16	800	2	1.25	98.61	74.74
9	Axial	440	6	0.50	61.32	90.34	600	1	0.50	93.03	80.68
10	Axial	616	6	1.25	92.90	86.70	600	3	1.25	96.12	67.73
11	Axial	264	6	1.25	79.04	89.28	600	2	1.25	47.36	86.26
12	Axial	440	8	1.25	90.41	86.48	600	2	1.25	95.13	72.32
13	Fact	616	4	0.50	38.55	89.22	400	1	0.50	14.97	89.88
14	Fact	264	4	0.50	23.99	91.38	800	1	0.50	61.24	82.87
15	Fact	616	4	2.00	75.55	87.36	400	3	2.00	13.50	87.98
16	Fact	616	8	2.00	98.23	84.64	800	3	2.00	56.22	78.42
17	Fact	616	8	0.50	77.18	85.62	400	1	0.50	97.17	75.71
18	Fact	264	4	2.00	51.55	88.74	800	1	2.00	87.04	63.35
19	Fact	264	8	0.50	48.25	89.38	400	3	0.50	79.76	69.31
20	Fact	264	8	2.00	80.90	88.94	600	3	2.00	86.23	79.10

where C_o and C_e are the liquid-phase concentrations at the initial state and at equilibrium (mg/L), respectively.

The effect of pH on metals removal was tested by varying the pH from 2 to 6, with initial metals concentration of 20 mg/L, carbon dosage 0.3 g, and adsorption temperature of 30°C. The initial pH of the metals solution was adjusted by addition of 0.10-M HCl or NaOH.

Equilibrium studies

In this study, adsorption isotherms were used to describe media performance and the relationship between adsorbent (MIOS and THOS) and dissolved adsorbate (Ni^{2+}) in solution. Adsorption experiments were carried out by mixing 100 mL of the synthetic wastewater with an initial Ni^{2+} concentration of 20 mg/L and a specific MIOS and THOS dose, that is, 0.025, 0.05, 0.1, 0.15, 0.2, 0.25, 0.3, 0.4, 0.5, 1.0, or 2.0 g. A shaking speed of 200 rpm and equilibrium period of 3 h were applied to ensure equilibrium conditions. The amount of adsorption at equilibrium, q_e (mg/g), was calculated by

$$q_{e} = \frac{(C_o - C_e)V}{W} \tag{5}$$

where C_o and C_e (mg/L) are the liquid-phase concentrations of Ni^{2+} at initial and equilibrium conditions, respectively, V (L) is the volume of the solution, and W (g) is the mass of dry MIOS or THOS used.

BET, SEM, and FTIR of the prepared activated carbon

The surface area, pore volume, and average pore diameter of the samples were determined by using Micromeritics ASAP 2020 volumetric adsorption analyzer. The BET surface area was measured from the adsorption isotherm using Brunauer-Emmett-Teller equation. The total pore volume was estimated to be the liquid volume of nitrogen at a relative pressure of 0.98. The surface morphology of the samples was examined using a scanning electron microscope (Quanta 450 FEG, Netherland). Chemical characteristics of surface functional group of the activated carbon was detected by diluting in K-Br pellets were recorded with FTIR spectroscope (IR Prestige 21 Shimadzu, Japan) in the 400–4000 cm^{-1} wave number range.

Desorption studies

The prepared carbon was saturated with a Ni^{2+} concentration of 20 mg/L until equilibrium was achieved. The concentration of adsorbate at the equilibrium C_e (mg/L) was calculated as the difference between the initial and equilibrium concentration ($C_0 - C_e$). The spent MIOS and THOS activated carbons were then separated from the solution and washed with deionized water to remove any unsorbed Ni^{2+}. The samples were dried in an oven and were then agitated with 0.1 M HCl for desorption studies. After desorption, the removal efficiencies of the regenerated media were examined by repeating the adsorption-desorption process five times. The recovery efficiency was calculated using Eq. (6)

$$\text{Recovery}\,(\%) = \frac{\text{Removal percentage of regenerated media}}{\text{Removal percentage of fresh media}} \times 100 \tag{6}$$

Results and Discussion

A total of 20 runs of the CCD experimental design were conducted. The results are shown in Table 2. The observed percent removal efficiencies varied between 23.99 and 98.23% for Ni^{2+} removal and 84.64 and 91.38% for MIOS yield. Comparing to THOS, the observed percent removal efficiencies varied between 13.50 and 99.43% for Ni^{2+} removal and 63.36 and 89.88% for THOS yield.

Analysis of variance

The results of second-order response surface models fitting in the form of ANOVA and other statistical parameters for Ni^{2+} removal and carbon yield by the two methods are given in Table 3. Data given in this table demonstrate that the two models were significant at the 5% confidence level, that is, P values < 0.05. The closer the R^2 to unity and the smaller the standard deviation, the more accurate the response could be predicted by the model.

The correlation coefficients obtained for Ni^{2+} removal and carbon yield obtained for the two models close to one demonstrates favorable agreement between the calculated and observed results within the experimental range. According to Bashir et al.[23] for a model to feature good fit, the correlation coefficient must be a minimum of 0.80.

The AP ratios of the models were varied between 39.60 and 49.71 for Ni^{2+} removal and 21.25 and 31.59 for carbon yield, which is an adequate signal for the models. AP values higher than 4 are desirable and confirm that the predicted models can be used to navigate the space defined by CCD.[23] The coefficient of variance (CV), which is calculated as the ratio of the standard error of the estimate to the mean value of the observed response (as a percentage), identifies the reproducibility of a model. A model is typically considered reproducible if its CV is not more than 10%.[24] According to Table 3, the CV values obtained for Ni^{2+} removal and MIOS yield were relatively small not exceeding 4.63%. In this study, four quadratic models were significant model terms (Table 3). Insignificant model terms, which have limited influence, were excluded from the study to improve the models. Based on the statistical results obtained, the aforementioned models were adequate to predict Ni^{2+} removal and carbon yield within the range of variables studied.

The final regression models, in terms of their coded factors, are expressed by the following second-order polynomial equations (Table 4).

Confirming whether or not the selected model provides adequate approximation of the real system is generally important. The model adequacy can be judged by applying the diagnostic plots provided by Design Expert 6.0.7 software, such as predicted vs. actual values plots. The plots of predicted vs. actual values for Ni^{2+} removal and carbon yield via microwave and thermal processes are shown in Figure 2. These plots show adequate agreement between real data and data gained from the models. Thus, all predictive models can be used to navigate the design space defined by CCD.

The perturbation plot (Figure 3) shows the comparative effects of all independent factors on Ni^{2+} removal and carbon yield by the two methods. In MIOS Figures 3a,b, a curvature in radiation power (X_1), radiation time (X_2), and impregnation ratio (X_3) shows that the responses of Ni^{2+} removal and MIOS yield are highly sensitive to these three process factors. For THOS Figure 3c, a curvature in activation temperature (X_1) and impregnation ratio (X_3) shows that the Ni^{2+} removal is highly sensitive to these two process factors. The relatively semiflat activation time (X_2) curve

Table 3. ANOVA Results and Adequacy of the Quadratic Models for Ni^{2+} Removal and Carbon Yield

Activation Method	Response	Source of Data	Sum of Squares	Degree of Freedom	Mean Square	F-Value	Prob. > F	Comments
Microwave	Ni removal (%)	Model	8078.44	5	1615.69	191.48	<0.0001	SD = 2.90,
		X_1	973.64	1	973.64	115.39	<0.0001	CV = 3.88,
		X_2	2185.34	1	2185.34	258.99	<0.0001	R^2 = 0.9856,
		X_3	2218.26	1	2218.26	262.89	<0.0001	Adj R^2 = 0.980;
		X_2^2	656.81	1	656.81	77.84	<0.0001	Adeq Precision = 49.71
		X_3^2	432.43	1	432.43	51.25	<0.0001	
		Residual	118.13	14	8.44	–	–	
		Lack of fit	116.31	9	12.92	35.56	–	
		Pure error	1.82	5	0.36	–	–	
	MIOS yield	Model	44.15	7	6.31	26.19	<0.0001	SD = 0.49,
		X_1	20.11	1	20.11	83.50	<0.0001	CV = 0.56,
		X_2	11.66	1	11.66	48.44	<0.0001	R^2 = 0.9386,
		X_3	6.40	1	6.40	26.58	0.0002	Adj R^2 = 0.902;
		X_2^2	2.02	1	2.02	8.37	0.0135	Adeq Precision = 21.25
		X_3^2	1.51	1	1.51	6.26	0.0278	
		X_1X_2	2.55	1	2.55	10.61	0.0069	
		X_2X_3	1.19	1	1.19	4.92	0.0465	
		Residual	2.89	12	0.24	–	–	
		Lack of fit	1.17	7	0.17	0.48	–	
		Pure error	1.72	5	0.34	–	–	
Thermal	Ni removal (%)	Model	14003.78	6	2333.96	169.44	<0.0001	SD = 3.71,
		X_1	1003.74	1	1003.74	72.87	<0.0001	CV = 4.63,
		X_2	46.75	1	46.75	3.39	0.0884	R^2 = 0.9874,
		X_3	6352.57	1	6352.57	461.18	<0.0001	Adj R^2 = 0.982,
		X_1^2	201.64	1	201.64	14.64	0.0021	Adeq Precision = 39.60
		X_3^2	2486.34	1	2486.34	180.50	<0.0001	
		X_1X_3	1073.14	1	1073.14	77.91	<0.0001	
		Residual	179.07	13	13.77	–	–	
		Lack of fit	178.43	8	22.3	173.53	–	
		Pure error	0.64	5	0.13			
	THOS yield	Model	1123.81	4	280.95	64.81	<0.0001	SD = 2.08,
		X_1	257.65	1	257.65	59.43	<0.0001	CV = 2.69,
		X_2	84.08	1	84.08	19.39	0.0005	R^2 = 0.9453,
		X_3	717.11	1	717.11	165.41	<0.0001	Adj R^2 = 0.931,
		X_2^2	64.97	1	64.97	14.99	0.0015	Adeq Precision = 31.59
		Residual	65.03	15	4.34	–	–	
		Lack of fit	63.71	10	6.37	24.1	–	
		Pure error	1.32	5	0.26	–	–	

shows less sensitivity of Ni^{2+} removal to alter with respect to change in activation time. In other words, the activation time has no important influence in the preparation process when compared to activation temperature and impregnation ratio. However, all independent factors have a significant effect on THOS yield as shown in Figure 3d.

Nickel removal efficiency and carbon yield

To assess the interactive relationships between independent factors and the responses of certain models, three-dimensional (3-D) surface response and contour plots utilizing Design Expert 6.0.7 software were constructed. As shown in Figures 4–6, in each plot, one variable was kept constant while the two others were varied within the experimental ranges for the two methods.

For microwave process, Figure 4 shows the 3-D response surface of the combined effects of radiation power and impregnation ratio when the radiation time was kept at optimum level ($t = 7$ min). The contour plots demonstrate that the improvement in removal efficiency of Ni^{2+} from 55.05 to 99.99% may be attributed to increases in radiation power and impregnation ratio (Figure 4a) and that the improvement in MIOS yields from 85.41 to 90.32% may be attributed to decreases in radiation power and impregnation ratio (Figure 4b). A possible explanation for this effect is that the reaction between KOH and the char is greater at higher-radiation power, thereby facilitating the development of the pore structure and resulting in the formation of a larger number of active sites. In addition, the removal of several components from the activation process, such as tar and volatile matter, is easier at higher-radiation power, which also promotes the activation process. Similar results have been obtained by other researchers.[9,14,25]

Figure 5 shows the 3-D response surface of the combined effect of radiation time and impregnation ratio, while the radiation power was kept at optimum level (power = 565

Table 4. Final Equations in Terms of Coded Factors

	Microwave	Thermal
Ni^{2+} removal (%)	$= +87.84 + 9.87\,X_1 + 14.78\,X_2 + 14.89\,X_3 - 14.33\,X_2^2 - 11.62\,X_3^2$	$= +98.09 + 10.02\,X_1 - 2.16\,X_2 + 25.20\,X_3 - 7.94\,X_1^2 - 27.87\,X_3^2 - 11.58\,X_1\,X_3$
Yield (%)	$= +88.34 - 1.42\,X_1 - 1.08\,X_2 - 0.80\,X_3 - 0.79\,X_2^2 + 0.69\,X_3^2 - 0.57\,X_1\,X_2 + 0.38\,X_2\,X_3$	$= +79.20 - 5.08\,X_1 - 2.90\,X_2 - 8.47\,X_3 - 3.60\,X_2^2$

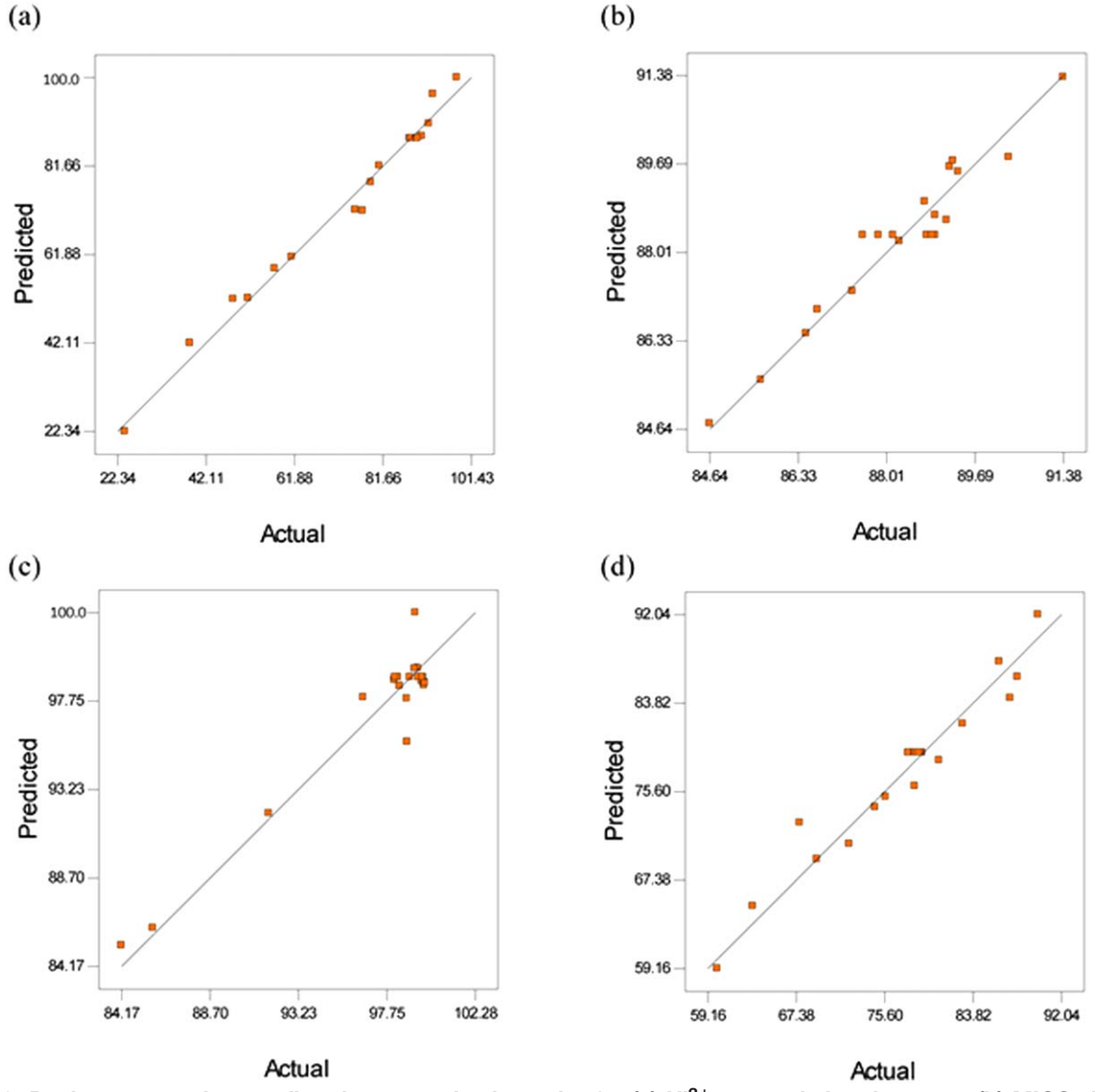

Figure 2. Design-expert plot; predicted vs. actual values plot for (a) Ni^{2+} removal via microwave (b) MIOS yield, (c) Ni^{2+} removal via thermal heating, and (d) THOS yield.

[Color figure can be viewed in the online issue, which is available at wileyonlinelibrary.com.]

W). The contour plots demonstrate that the improvement in removal efficiency of Ni^{2+} may be attributed to increases in radiation time and impregnation ratio (Figure 5a) and that the improvement in MIOS yield may be attributed to decreases in radiation time and impregnation ratio (Figure 5b). The activation degree significantly depended on radiation time. A possible explanation for this result is that with increased radiation time, significantly more pores and active sites develop on the MIOS surface. Therefore, the removal efficiency of MIOS increases (Figure 5a) and the yield decreases (Figure 5b) with increasing radiation time. Similar results were obtained by other researchers.[9,14,25,26]

For thermal process, Figure 6 shows the 3-D response surface of the combined effects of temperature and impregnation ratio when the time was kept at optimum level ($t = 2$ h). The contour plots demonstrate that the improvement in removal efficiency of Ni^{2+} may be attributed to increases in temperature and impregnation ratio (Figure 6a) and that the improvement in THOS yield may be attributed to decreases in radiation power and impregnation ratio (Figure 6b). The maximum observed removal rate of Ni^{2+} was 99.99% at a temperature of 715°C and impregnation ratio of 1.53.

Solution pH also affects adsorption by regulating the adsorbent surface charge as well as degree of ionization of the adsorbate molecules. The percentage of Ni^{2+} removal using OS activated carbon were found to increase significantly with the increase in solution pH from 3 to 6 and the highest metals removals were achieved at pH 5. According to Božić et al.[27] at low pH < 3 the minimal removal may be an effect of the higher concentration and high mobility of the H^+, which competes with metal ions on the active sites on the sorbent surface, resulting in its preferential adsorption rather than the metal ions. Therefore, H^+ ions react with anionic functional groups on the surface of OS activated carbon and results in the reduction of the number of binding sites available for the adsorption of Ni^{2+}. This increase may has been an effect of the presence of negative charge on the surface of the adsorbent that may has been responsible for the

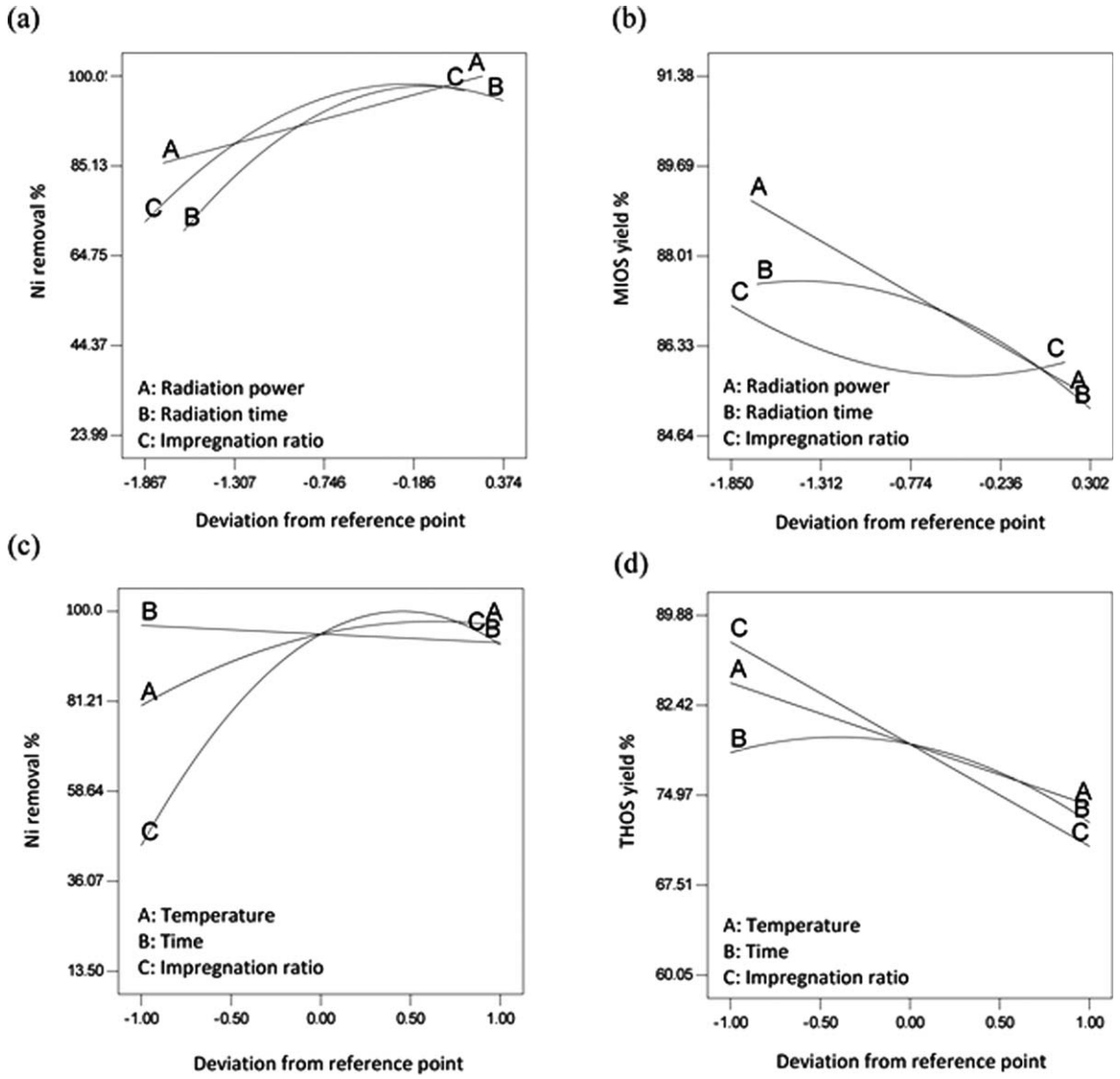

Figure 3. Perturbation plot for (a) Ni^{2+} removal by MIOS, (b) MIOS yield, (c) Ni^{2+} removal by THOS, and (d) THOS yield.

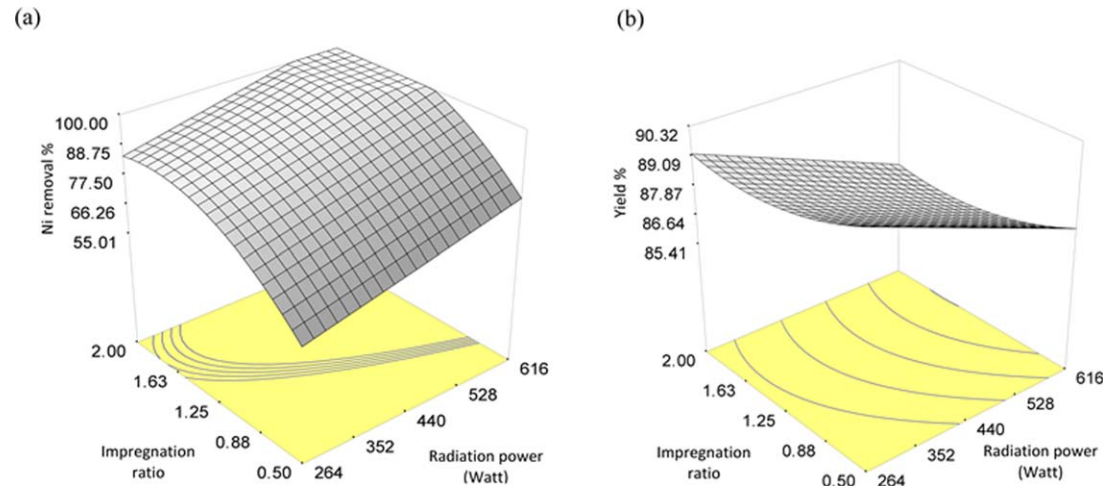

Figure 4. Three-dimensional response surface plot: (a) Ni^{2+} removal by MIOS, and (b) MIOS yield (effect of radiation power and chemical impregnation ratio, $t = 7$ min).

[Color figure can be viewed in the online issue, which is available at wileyonlinelibrary.com.]

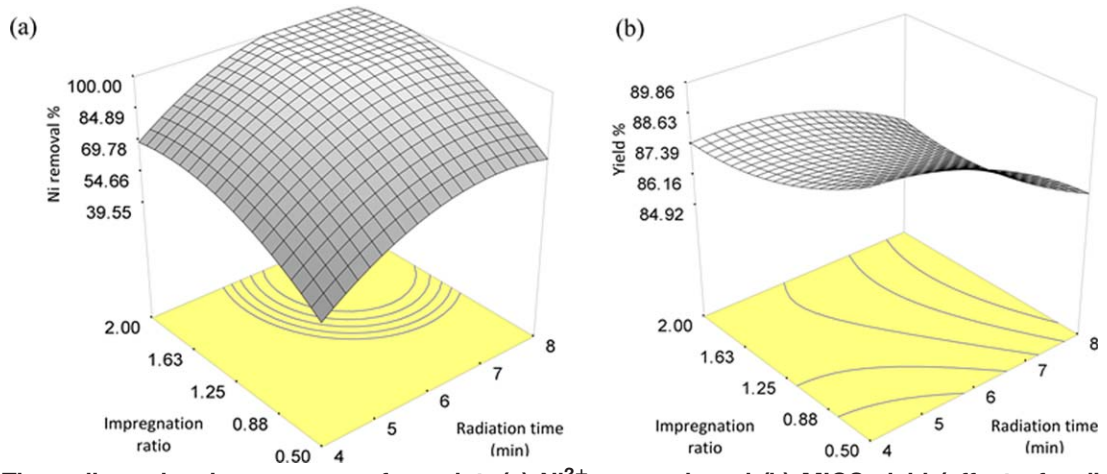

Figure 5. Three-dimensional response surface plot: (a) Ni^{2+} removal, and (b) MIOS yield (effect of radiation time and chemical impregnation ratio, radiation power = 565 W).

[Color figure can be viewed in the online issue, which is available at wileyonlinelibrary.com.]

metal binding because solution pH can affect the charge of OS activated carbon surfaces.[28] In addition, at higher pH values, the lower number of H^+ and greater number of ligands with negatives charges result in greater metal adsorption. The same trend was observed by several researchers who studied metal sorption by different biomaterials, namely, copper by sawdust,[29] lead and cadmium by Garcinia mangostana,[30] cadmium by orange wastes.[31]

Comparison of the two techniques

An attempt to compare the activated carbon prepared using the thermal and microwave-assisted heating in terms of the preparation conditions, characteristics, adsorption capacities, and removal efficiencies is the focus of this work.

Comparison on optimization conditions

Optimization was carried out to determine the optimum MIOS and THOS preparation conditions for the optimal removal of Ni^{2+} from synthetic wastewater and carbon yield using Design Expert 6.0.7 software. According to the software optimization step, the desired goal for each operational condition (radiation power/temperature, time, and impregnation ratio) was selected to be "within" the range. The responses (Ni^{2+} removal and carbon yield) were defined as maximum to achieve the highest performance. The obtained value of desirability (0.99) showed that the estimated function represents the experimental model and desired conditions. The predicted results of Ni^{2+} removal and carbon yield obtained at optimum conditions are listed in Table 5. As shown in Table 5, 99.99% Ni^{2+} removal and 74.79% THOS yield were predicted according to the model under optimized preparation conditions (temperature of 715°C, time of 120 min, and impregnation ratio of 1.53). For microwave process, 99.99% Ni^{2+} removal and 86.05% MIOS yield were predicted according to the model under optimized preparation conditions (radiation power of 565 W, radiation time of 7 min, and impregnation ratio of 1.87). In this study, a shorter preparation time was applied by microwave compared to thermal and with that used microwave in the literature.[9,15,26]

Comparison on characteristics of optimized MIOS and THOS

The BET surface area, mesopore surface area, total pore volume, and average pore diameter of the MIOS were 1280.71 m^2/g, 883.49 m^2/g, 0.604 cm^3/g, and 4.63 nm, respectively. According to the results in Table 6, the

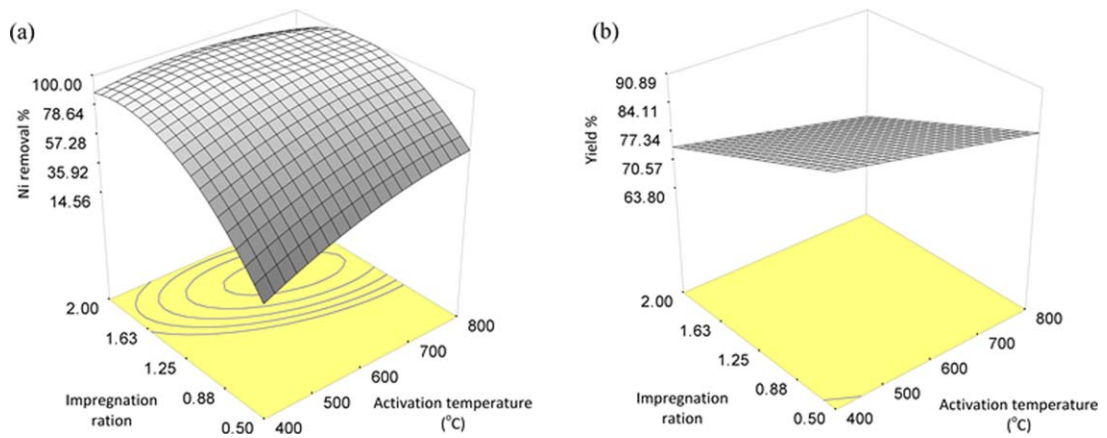

Figure 6. Three-dimensional response surface plot: (a) Ni^{2+} removal by THOS, and (b) THOS yield (effect of temperature and chemical impregnation ratio, t = 2 h).

[Color figure can be viewed in the online issue, which is available at wileyonlinelibrary.com.]

Table 5. Optimization Results for Maximum Ni^{2+} Removal and Carbon Yield Predicted By the Two Methods

Activation Method	Power (W)/Temp. (°C)	Time (min)	Impregnation Ratio	Ni^{2+} Removal (%)	Carbon Yield (%)	Desirability
Microwave	565	7	1.87	99.99	86.05	0.99
Thermal	715	120	1.53	99.99	74.79	

microwave-activated carbon exhibited a slightly higher portion of mesopores (833.49 m^2/g) than the thermally activated carbons (740.66 m^2/g), probably because the activation reaction under microwave radiation was more intense. A much shorter activation time was required for microwave activation, which was one of its advantages as also demonstrated in previous works.[9,26] A high temperature, perhaps above 1000°C, could be reached quickly under microwave radiation,[32] which enhanced the development of the pore structure. Another reason should be attributed to the distinct mechanism of microwave heating. The interior part of the carbon can be heated more favorably under microwave radiation, creating a temperature gradient reducing from the center to the surface. As a consequence, the release of tar or volatile matter would be promoted.

Compared to the thermal method, the microwave-induced activation also brought about higher carbon yield, although the difference was not so significant. It was possibly because that in the thermal method long activation time needed that increased the weight loss of the carbon precursor, while in the microwave activation due to a shorter activation time the weight loss was alleviated.

The textural structures of the THOS and MIOS were evaluated through SEM, as depicted in Figure 7. The SEM images indicated good organization and uniform porosity, large and well distribution of pores, and a series of irregular cavitation distributed around the surface can be observed on the sample surface of THOS and MIOS. It can be seen that conventional and microwave assisted activation transforms the agricultural derives chars into a well pronounced and developed pores over the surface, indicating good possibility for the heavy metals to be adsorbed (Figures 7c,d). The pore developed over the surface of THOS was composed of a series of uniform and circular pores, forming an orderly pore structure (Figure 7c), while the surface of MIOS was hexagonal in shape and arranged in an array of honey-comb structure (Figure 7d).

The obtained FTIR spectrum of MIOS and THOS (Figure 8) revealed the peaks between 3861–3734, 2411–2098, 1905–1886, 1762–1242, and 999–590 cm^{-1}, which corresponds to the presence of —OH (hydroxyl), C≡C (alkynes), —COOH (carboxylic acids), in-plane —OH, and C—O—C (esters, ether or phenol) functional groups. Based on experimental results and the speciation of metal ions, Ni^{2+} removal by MIOS and THOS may has occurred through the complexation between the negatively charged functional groups, such as carboxylic groups (—COOH) and hydroxyl groups (—OH),[31,33] and metal cations, such as Me^{+2} and $Me(OH)^{+}$. At pH higher than 3–5, carboxylic groups are deprotonated and negatively charged. Accordingly, the attraction of positively charged metal ions would be improved.[34] In other words, the adsorptive characteristic was influenced by the surface functionalities, which may serve as the chemical binding sites for the adsorption process. Besides, the presence of hydroxyl, carbonyl, and alkyl groups could dissociate as negatively charge sites, and contributing to electrostatic attraction between the activated carbons and the positively charge metal ions.[35,36]

Comparison on materials consumption

Materials consumption (power, nitrogen gas, and chemical) estimates per kg of activated carbon prepared via microwave and conventional thermal process were calculated based on the optimum preparation condition Table 4. The carbonization step was carried out at 600°C for 1 h for both MIOS and THOS. The activation step for MIOS was at power level 565 W and time 7 min, while for THOS was at temperature 715°C and time 2 h. According to Table 7, the calculated total power consumption of the preparation process was 19.40 KWh/kg for MIOS and 61.60 KWh/kg for THOS. Thus, power consumption for preparing 1 kg of activated carbon by THOS was three times higher than MIOS process rendering the process via microwave more economical for power consumption than the conventional heating. Furthermore, the gas consumption for preparing 1 kg of activated carbon by THOS (36 L) was two times higher than MIOS process (17.5 L) based on 150 and 300 mL/min gas flow rate respectively. Meanwhile, the chemical (KOH) consumption by MIOS (1.87 kg/kg) was slightly higher than THOS (1.53 kg/kg) process. This findings implies the material consumed to prepare 1 Kg of activated carbon by the MIOS was lower than the THOS, rendering the preparation process via microwave is more economical compared to conventional heating.

Comparison on adsorption capacities

Adsorption Isotherms. Equilibrium isotherms in this study were analyzed using Langmuir and Freundlich isotherms as the most frequently used models for describing the adsorption characteristics of the THOS and MIOS that were used in Ni^{2+} synthetic wastewater treatment.

Langmuir isotherm.

$$\frac{1}{(q_e)} = \frac{1}{QbC_e} + \frac{1}{Q} \tag{7}$$

Freundlich isotherm.

$$\log q_e = \log K + \frac{1}{n}\log C_e \tag{8}$$

Table 6. Activation Effects of Microwave and Conventional Thermal Processes

Sample	BET Surface Area (m^2/g)	Mesopore Surface Area (m^2/g)	Total Pore Volume (cm^3/g)	Average Pore Diameter (nm)	Yield (%)
MIOS	1280.71	883.49	0.604	4.63	86.05
THOS	886.72	740.66	0.507	4.22	74.79

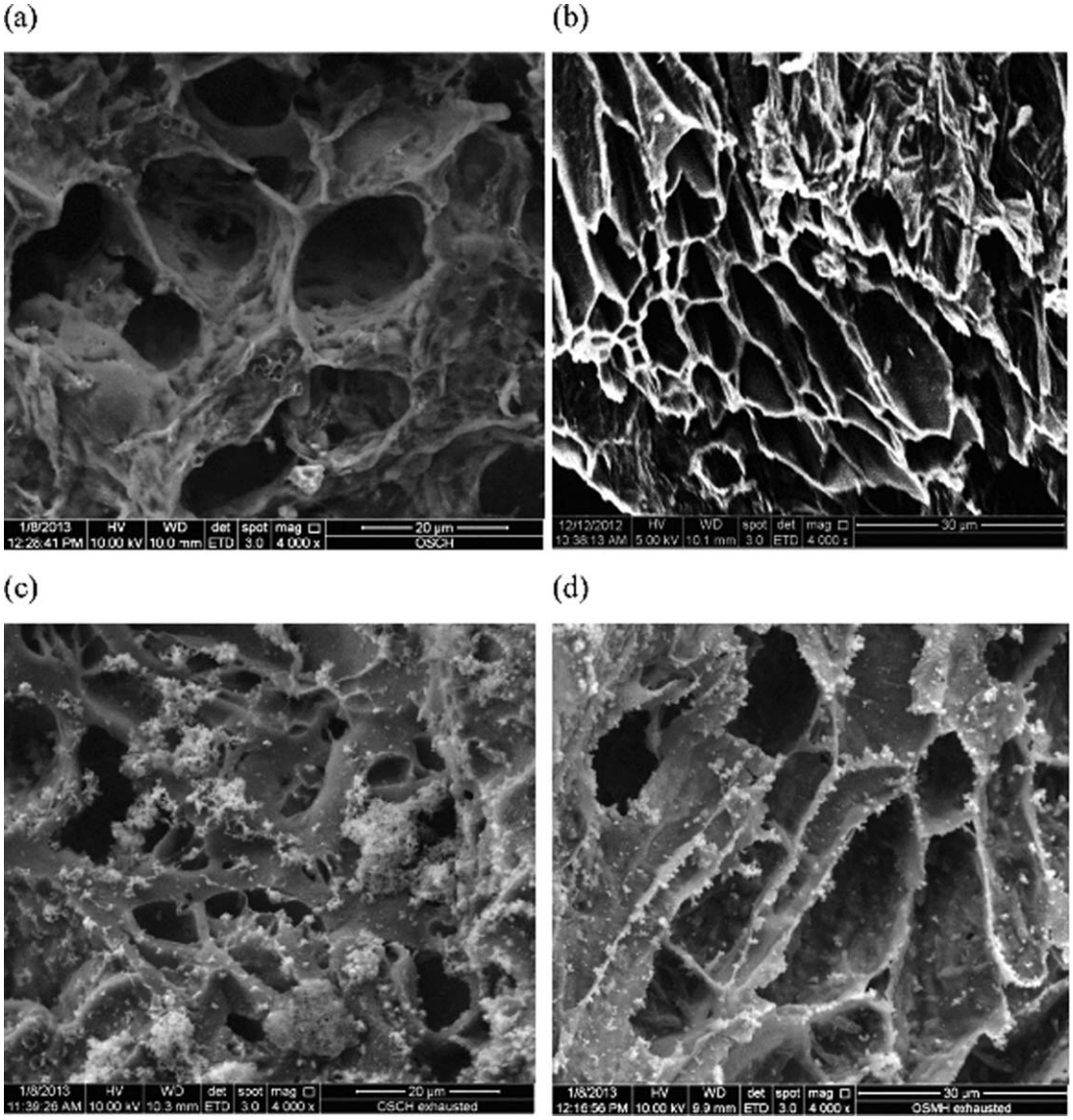

Figure 7. Scanning electron micrograph of the OS derived: (a) THOS, (b) MIOS, (c) THOS after Ni adsorption, and (d) MIOS after Ni adsorption (magnifications: 4000×).

where, q_e (mg/g) is the amount of adsorbed metal ions per unit weight of adsorbent at equilibrium concentration, C_e (mg/L). The Q (mg/g) and b (L/mg) are the Langmuir constants related to the maximum monolayer capacity and energy of adsorption, respectively. The K and $1/n$ are Freundlich constants related to adsorption capacity and intensity of adsorption respectively.

Table 8 shows that the Langmuir isotherm fits the data better than the Freundlich isotherm. This result is also confirmed by the high R^2 of the Langmuir model (0.991 and 0.990) compared to that of the Freundlich model (0.894 and 0.905), indicating that Ni^{2+} adsorption on MIOS and THOS occurs as monolayer adsorption on a surface that is homogeneous in adsorption affinity.[37] Thus, the adsorption isotherm data were best described by the Langmuir isotherm and the adsorption capacity was determined to be 12.0 and 8.42 mg/g for MIOS and THOS, respectively, indicating that MIOS has a higher adsorption capacity compared to THOS.

The adsorption capacities of MIOS and THOS for other heavy metal ions which studied elsewhere[38,39] were in the order $Fe^{2+} > Pb^{2+} > Cu^{2+} > Zn^{2+} > Ni^{2+} > Cd^{2+}$. The results obtained agreed with those of the study of Li et al.,[40] in which the following order for the sorption of metals onto sawdust and modified peanut husk was reported: $Pb^{2+} > Cu^{2+} > Cr^{6+}$. The next, by Xie et al.,[41] found a similar order of affinity: $Pb^{2+} > Cu^{2+} > Cd^{2+}$ onto sewage sludge activated carbon. Further, by Brown et al.[42] examined peanut hull pellets and found a similar order of affinity: $Pb^{2+} > Zn^{2+} > Cu^{2+} > Cd^{2+}$. Spinti et al.[43] reported a similar order of affinity for immobilized biomass (peat) beads: $Fe^{2+} > Al^{3+} > Cu^{2+} > Cd^{2+}$, Zn^{2+}. Another study by Tuzen et al.[44] reported that, the affinity order of the metal ions toward carbon nanotubes was $Cu^{2+} > Pb^{2+} > Zn^{2+} > Co^{2+} > Ni^{2+} > Cd^{2+} > Mn^{2+}$. Another study by Reddad et al.[45] investigated sugar beet pulp and found a similar order of affinity: $Pb^{2+} > Cu^{2+} > Zn^{2+} > Cd^{2+} > Ni^{2+}$.

According to Lim et al.,[46] the heavy metal's electronegativity and its ionic radius along with other factors such as solution pH might affect the metal's affinity to be adsorbed by activated carbon. Electronegativity represents the metal ion attraction to the negatively charged sites. The electronegativity of Pb^{2+}, Fe^{2+}, Cu^{2+}, Zn^{2+}, Ni^{2+}, and Cd^{2+} are

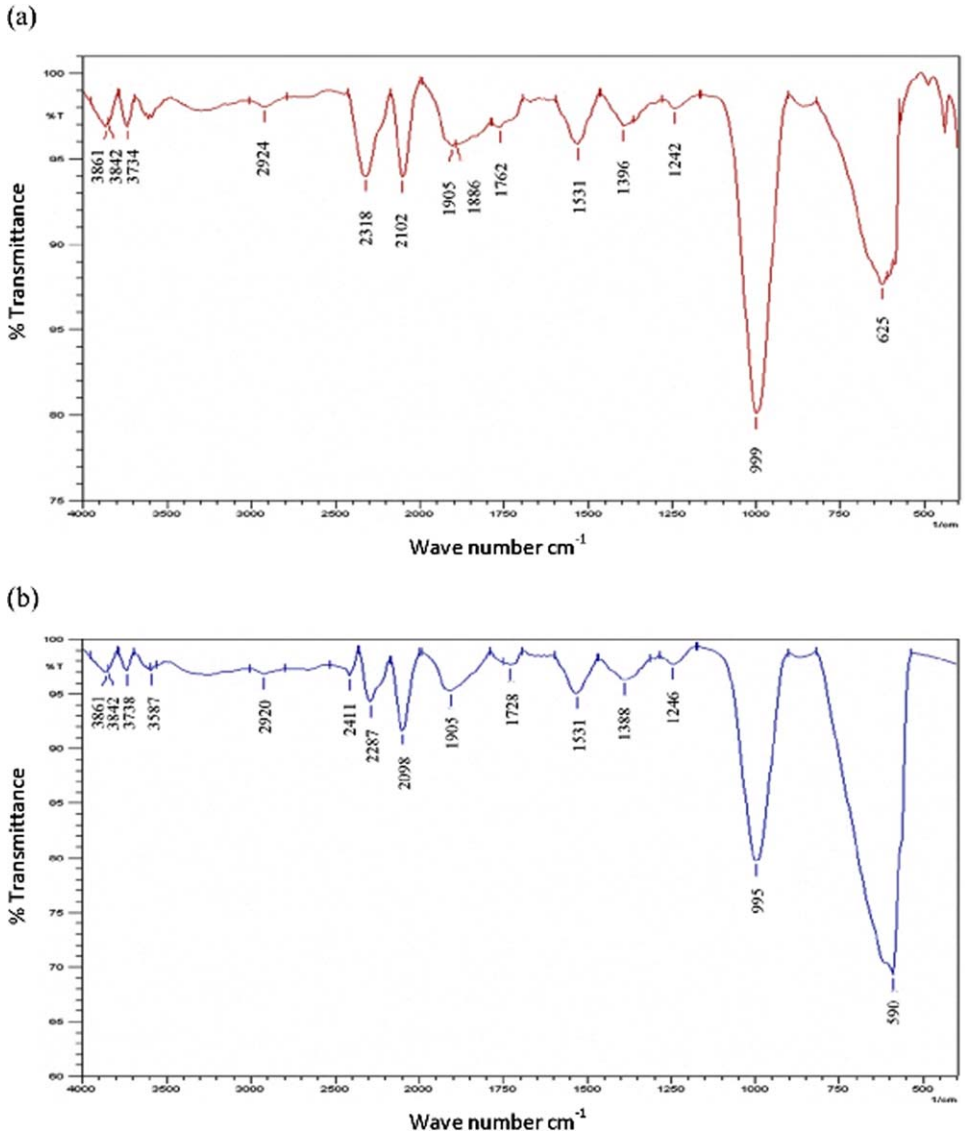

Figure 8. FTIR spectrums; (a) MIOS and (b) THOS.

[Color figure can be viewed in the online issue, which is available at wileyonlinelibrary.com.]

2.33, 1.83, 1.9, 1.65, 1.91, and 1.69, respectively. As a general trend, higher electronegativity corresponds to a higher sorption level of the metal ion.[44] It can be noted that Pb^{2+} has the highest electronegativity compared to other metal ions meanwhile Zn^{2+} and Cd^{2+} have the lowest electronegativity. It is also known that the adsorption of any heavy metal with a smaller ionic radius is greater than that with a larger ionic radius. This is due to smaller radii metal ions have more accessibility to the surface and pores of the adsorbents than the bigger ones.[41] The ionic radii of the metals, namely, Fe^{2+}, Ni^{2+}, Cu^{2+}, Zn^{2+}, Cd^{2+}, and Pb^{2+} are 0.64, 0.69, 0.73, 0.74, 0.97, and 1.19 A°, respectively. It can be noted that Pb^{2+} and Cd^{2+} have the largest ionic radius compared to other metal ions meanwhile Fe^{2+} has the smallest ionic radius. Based on research results, Fe^{2+} has the highest adsorption affinity compared to other metals due to combination of small ionic radius and high electronegativity. Meanwhile, Cd^{2+} has the lowest adsorption affinity compared to other heavy metals due to its large ionic radius and low electronegativity. As mentioned in effect of initial solution pH, the pH of the aqueous solution is an important parameter controlling the adsorption process. The increase in solution pH leads to the increase in the presence of negative charge on the activated carbon surface which responsible for the heavy metals binding.[28] Aforementioned, the adsorption selectivity is a combined action of electronegativity, ionic radius, pH, and other factors. Thus, the sorption depends not only on specific surface area, pH, and surface functional groups but also metal ions to be adsorbed.[36]

Table 7. Comparison of the Activated Carbon Power Consumption via Microwave and Conventional Thermal Processes

	Preparation Method	
Parameters	Thermal	Microwave
Electricity consumed (Kw) for carbonize 1 Kg of OS	18.48	18.48
Electricity consumed (Kw) for activate 1 Kg of char	43.12	0.917
Total Electricity consumed (Kw) for prepare 1 Kg of activated carbon	61.60	19.40

Table 8. Langmuir and Freundlich Isotherm Parameters for Ni^{2+} Adsorption onto MIOS and THOS

	Langmuir Isotherm Model				Freundlich Isotherm Model		
Parameter	Q (mg/g)	b (L/mg)	R^2	R_L	K (mg/g) (L/mg)$^{1/n}$	$1/n$	R^2
MIOS	12.0	3.051	0.991	0.02	8.33	0.144	0.894
THOS	8.42	5.094	0.990	0.01	6.41	0.137	0.905

Table 9 lists the comparison of Ni^{2+} adsorption for various activated carbons. The results obtained in this work were comparable to the works reported in the literature. The variation in the Ni^{2+} adsorption might be due to the different precursors as well as the activation methods and/or conditions used to prepare the activated carbons.

Adsorption Kinetics. Adsorption kinetics is highly significant in evaluating the performance of a certain adsorbent and understanding the underlying mechanisms of adsorption.[47] In this study, the kinetic modeling of Ni^{2+} adsorption on MIOS and THOS were investigated using two common models, namely, the pseudofirst-order and pseudosecond-order models. The pseudofirst-order model is illustrated as follows

$$\log (q_{e-}q_t)=\log (q_e)-\frac{K_1 t}{2.303} \tag{9}$$

A pseudosecond-order model is described as follows.

$$\frac{t}{q_t}=\frac{1}{k_2 q_e^2}+\frac{t}{q_e} \tag{10}$$

where q_e and q_t (mg/g) are the amounts of adsorbate adsorbed at equilibrium and at any time, t (h), respectively, k_1 (1/h), and k_2 (g/mg h) are the equilibrium rate constants of pseudofirst-order and pseudosecond-order models, respectively, and t (h) is the contact time. The linear plot of log ($q_e - q_t$) vs. t provides a slope of k_1 and intercept of log q_e.

The values of k_1 and R^2 obtained from the plot for Ni^{2+} adsorption on the adsorbent are shown in Table 10. The R^2 values (0.945 and 0.955) obtained for the pseudofirst-order model were not high and the experimental q_e did not agree with the calculated value obtained from the plots. These findings show that Ni^{2+} adsorption on the adsorbent (MIOS and THOS) does not follow a pseudofirst-order kinetic model.

Meanwhile, the R^2 (0.997 and 0.995) values obtained from the pseudosecond-order model were close to unity, indicating that Ni^{2+} adsorption on MIOS and THOS fits this model well and that the adsorption process is controlled by chemisorption.[31]

Desorption and Repeated Use. The influence of recycling times or reuse of MIOS and THOS on the recovery efficiencies of Ni^{2+} was studied. Desorption studies of the Ni^{2+} were carried out in five cycles with different concentrations of HCl solutions, which has been reported to be an efficient metal desorbent.[48] The desorption of metal ions was found to be more effective by using 0.1 M HCl solution. The H^+ from HCl easily displaces metal ions bonded to the adsorbent during the desorption stage. After five cycles, recovery efficiency of activated carbon decreased from 99.74 to 93.47% and 99.98 to 92.90% for Ni^{2+} removal using MIOS and THOS, respectively. It can be concluded that the MHOS and THOS can be used for several times without significantly decreasing its recovery efficiencies. However, the changes in mesoporous-microporous structures of the activated carbons during the regeneration process,[49] weight losses for several time of regeneration,[50] and the pore blockage as a consequence of the incomplete adsorption of metals molecules retained in the carbon network[51,52] might responsible for the decreases in recovery efficiency.

Conclusions

In this study, conventional and microwave heating systems for the preparation of activated carbon form OS with KOH activation agent are compared for removing Ni^{2+}, and carbon yield and the results are as follows:

i. The optimal activated carbon in conventional heating was obtained at 715°C, 2 h activation time, and 1.53 impregnation ratio. Meanwhile, the optimum conditions using microwave heating were radiation power of 565 W, radiation time of 7 min, and impregnation ratio of 1.87. The carbon yields using both MIOS and THOS were 86.05 and 74.79% respectively. The removal efficiency of Ni^{2+} was more than 99% indicating that activated carbon prepared from OS waste can be used for the treatment of wastewaters contaminated with heavy metals.

ii. The activated carbon prepared via microwave not only required a much shorter activation time compared to conventional thermal method, but also it resulted in higher yield and surface area with a better textural characteristic suggesting that the activation reaction under microwave radiation was more intense.

Table 9. Comparison of the Biosorption Capacity of Different Biosorbents

Sorbent	Activation Method	Adsorption Capacity (mg/g)	C_o	pH	Ref.
Bagasse fly ash	Conventional heating	1.12	12–14	6.0–6.5	[37]
Turkish fly ashes	Conventional heating	0.48	25	6.0	[38]
Sphagnum Moss Peat	Conventional heating	2.15	25	5.0	[39]
Petiolar felt-sheath of palm	Conventional heating	6.89	100	5.0	[40]
Jute fibers	Conventional heating	3.37	75	5.5	[41]
Clinoptilolite (zeolites)	–	0.9	10	4.0–5.0	[42]
Olive stone	Conventional heating	8.42	20	5.0	This work
Rice husk	Microwave heating	1.17	6	–	[5]
Olive stone	Microwave heating	12.0	20	5.0	This work

Table 10. Pseudofirst order and pseudosecond order kinetic model parameters for Ni^{2+} adsorption onto MIOS and THOS at a concentration of 20 mg/L

		PseudoFirst Order Model			PseudoSecond Order Model		
Parameter	$q_{e,\ exp}$ (mg/g)	K_1 (1/h)	$q_{e,\ cal}$ (mg/g)	R^2	K_2 (g/mg h)	$q_{e,\ cal}$ (mg/g)	R^2
MIOS	7.830	1.730	5.810	0.945	0.378	8.489	0.997
THOS	6.515	1.309	5.443	0.955	0.354	7.179	0.995

iii. For both methods, adsorption equilibrium data were fitted to the Langmuir isotherm model, with the monolayer adsorption capacities of 12.0 and 8.42 mg/g for MIOS and THOS, respectively, indicating that MIOS has a higher adsorption capacity compared to THOS due to higher BET surface area and pore volume especially for those contributed by the mesopores. Kinetics data were fitted to the pseudo second-order kinetics models.

iv. The comparative effects of all preparation factors on the responses demonstrated that the activation temperature and impregnation ratio were higher significant factors on Ni^{2+} removal for the prepared activated carbon via conventional thermal compared to activation time. Meanwhile, radiation power, radiation time, and impregnation ratio were the decisive factors affecting on Ni^{2+} removal for the prepared activated carbon via microwave heating. However, all preparation factors have a significant effect on carbon yields via both conventional and microwave heating.

v. Desorption of the metal ions was carried out using 0.1 M HCl and the repeated adsorption-desorption study showed that the adsorbent MHOS and THOS can be effectively used as an adsorbent for the removal of heavy metal ions from contaminated effluents.

vi. In microwave heating, the activation time, power consumption, and nitrogen flow are significantly lower than the conventional heating rendering the process via microwave more economical than the conventional heating.

Finally, the results proved that activated carbon prepared from OS waste can be used for the treatment of wastewaters contaminated with heavy metals. The lower holding time and better adsorption capacity of the activated carbon using microwave heating is well suited for commercial manufacture, as it would significantly improve the process economics due to time saving and low consumption of gas and energy compared to the conventional heating methods.

Acknowledgments

The authors wish to acknowledge the Universiti Sains Malaysia (USM) for its financial support under the USM and TWAS Fellowship scheme and RU-PRGS grant scheme (No. 8045048) and acknowledge Ministry of Higher Education, Malaysia for providing LRGS grant No. (203/PKT/670006) and (03-01-05-SF0502) to conduct this study.

Literature Cited

1. Verlicchi P, Galletti A, Petrovic M, Barceló D. Hospital effluents as a source of emerging pollutants: An overview of micropollutants and sustainable treatment options. *J Hydrol.* 2010;389(3–4):416–428.
2. Guijarro-Aldaco A, Hernández-Montoya V, Bonilla-Petriciolet A, Montes-Morán MA, Mendoza-Castillo DI. Improving the adsorption of heavy metals from water using commercial carbons modified with egg shell wastes. *Ind Eng Chem Res.* 2011;50(15):9354–9362.
3. Alslaibi TM, Abustan I, Ahmad MA, Foul AA. Cadmium removal from aqueous solution using microwaved olive stone activated carbon. *J Environ Chem Eng.* 2013;1(3):589–599.
4. Alslaibi TM, Abustan I, Ahmad MA, Abu Foul A. Kinetics and equilibrium adsorption of iron (II), lead (II), and copper (II) onto activated carbon prepared from olive stone waste. *Desalination Water Treat.* In press. DOI:10.1080/19443994.2013.833875.
5. Fu F, Wang Q. Removal of heavy metal ions from wastewaters: a review. *J Environ Manage.* 2011;92(3):407–418.
6. Alslaibi TM, Abustan I, Ahmad MA, Abu Foul A. Review: comparison of agricultural by-products activated carbon production methods using surface area response. *Caspian J Appl Sci Res.* 2013;2:18–27.
7. Alslaibi TM, Abustan I, Ahmad MA, Abu Foul A. A review: production of activated carbon from agricultural byproducts via conventional and microwave heating. *J Chem Technol Biotechnol.* 2013; 88(7):1183–1190.
8. Ahmad A, Hameed B. Effect of preparation conditions of activated carbon from bamboo waste for real textile wastewater. *J Hazard Mater.* 2010;173(1–3):487–493.
9. Liu QS, Zheng T, Wang P, Guo L. Preparation and characterization of activated carbon from bamboo by microwave-induced phosphoric acid activation. *Ind Crops Prod.* 2010;31(2):233–238.
10. Auta M, Hameed B. Optimized waste tea activated carbon for adsorption of Methylene Blue and Acid Blue 29 dyes using response surface methodology. *Chem Eng J.* 2011;175:233–243.
11. Yahaya N, Latiff M, Abustan I, Ahmad MA. Effect of preparation conditions of activated carbon prepared from rice husk by $ZnCl_2$ activation for removal of Cu(II) from aqueous solution. *Int J Eng Technol.* 2010;10(06):27–31.
12. Hameed B, Tan I, Ahmad A. Optimization of basic dye removal by oil palm fibre-based activated carbon using response surface methodology. *J Hazard Mater.* 2008;158(2):324–332.
13. Foo K, Hameed B. Preparation and characterization of activated carbon from pistachio nut shells via microwave-induced chemical activation. *Biomass Bioenergy.* 2011;35(7):3257–3261.
14. Deng H, Zhang G, Xu X, Tao G, Dai J. Optimization of preparation of activated carbon from cotton stalk by microwave assisted phosphoric acid-chemical activation. *J Hazard Mater.* 2010;182(1-3): 217–224.
15. Foo K, Hameed B. Preparation of activated carbon from date stones by microwave induced chemical activation: Application for methylene blue adsorption. *Chem Eng J.* 2011;170(1):388–341.
16. Foo K, Hameed B. Factors affecting the carbon yield and adsorption capability of the mangosteen peel activated carbon prepared by microwave assisted K_2CO_3 activation. *Chem Eng J.* 2011;180:66–74.
17. Foo K. Preparation and Characterization of Agricultural Waste Based Activated Carbons by Microwave-Induced Chemical Activation for the Adsorption of Methylene Blue. Malaysia: Universiti Sains Malaysia, 2012.
18. Rosli NA. Preparation of Activated Carbon from Fruit Waste for Dyes Removal: Equilibrium, Kinetic and Thermodynamic Studies. PhD Thesis. Malaysia: Universiti Sains Malaysia, 2012.
19. Yang J, Qiu K. Experimental design to optimize the preparation of activated carbons from herb residues by vacuum and traditional $ZnCl_2$ chemical activation. *Ind Eng Chem Res.* 2011;50(7):4057–4064.
20. Xin-hui D, Srinivasakannan C, Jin-hui P, Li-bo Z, Zheng-yong Z. Comparison of activated carbon prepared from Jatropha hull by conventional heating and microwave heating. *Biomass Bioenergy.* 2011; 35(9):3920–3926.
21. Alslaibi TM, Abustan I, Ahmad MA, Abu Foul A. Effect of different olive stone particle size on the yield and surface area of activated carbon production. *Adv Mater Res.* 2013;626:126–130.
22. Kumar R, Singh R, Kumar N, Bishnoi K, Bishnoi NR. Response surface methodology approach for optimization of biosorption process

for removal of Cr(VI), Ni(II) and Zn(II) ions by immobilized bacterial biomass sp. *Bacillus brevis*. *Chem Eng J*. 2009;146(3):401–407.
23. Bashir MJK, Aziz HA, Yusoff MS, Adlan MN. Application of response surface methodology (RSM) for optimization of ammoniacal nitrogen removal from semi-aerobic landfill leachate using ion exchange resin. *Desalination* 2010;254(1):154–161.
24. Beg QK, Sahai V, Gupta R. Statistical media optimization and alkaline protease production from Bacillus mojavensis in a bioreactor. *Process Biochem*. 2003;39(2):203–209.
25. Foo K, Hameed B. Preparation, characterization and evaluation of adsorptive properties of orange peel based activated carbon via microwave induced K_2CO_3 activation. *Bioresource Technol*. 2012; 104:679–686.
26. Deng H, Yang L, Tao G, Dai J. Preparation and characterization of activated carbon from cotton stalk by microwave assisted chemical activation-Application in methylene blue adsorption from aqueous solution. *J Hazard Mater*. 2009;166(2-3):1514–1521.
27. Božić D, Stanković V, Gorgievski M, Bogdanović G, Kovačević R. Adsorption of heavy metal ions by sawdust of deciduous trees. *J Hazard Mater*. 2009;171(1):684–692.
28. Mouni L, Merabet D, Bouzaza A, Belkhiri L. Adsorption of Pb(II) from aqueous solutions using activated carbon developed from Apricot stone. *Desalination* 2011;276(1):148–153.
29. Agouborde L, Navia R. Heavy metals retention capacity of a nonconventional sorbent developed from a mixture of industrial and agricultural wastes. *J Hazard Mater*. 2009;167(1):536–544.
30. Zein R, Suhaili R, Earnestly F, Munaf E. Removal of Pb(II), Cd(II) and Co(II) from aqueous solution using Garcinia mangostana L. *fruit shell*. *J Hazard Mater*. 2010;181(1):52–56.
31. Pérez-Marín AB, Zapata VM, Ortuño JF, Aguilar M, Sáez J, Lloréns M. Removal of cadmium from aqueous solutions by adsorption onto orange waste. *J Hazard Mater*. 2007;139(1):122–131.
32. Liu X, Quan X, Bo L, Chen S, Zhao Y, Chang M. Temperature measurement of GAC and decomposition of PCP loaded on GAC and GAC-supported copper catalyst in microwave irradiation. *Appl Catal A: General*. 2004;264(1):53–58.
33. Norton L, Baskaran K, McKenzie T. Biosorption of zinc from aqueous solutions using biosolids. *Adv Environ Res*. 2004;8(3):629–635.
34. Ho Lee S, Hun Jung C, Chung H, Yeal Lee M, Yang JW. Removal of heavy metals from aqueous solution by apple residues. *Process Biochem*. 1998;33(2):205–211.
35. Mohammad M. Studies on the Adsorption of Heavy Metal Ions and Dye from Aqueous Solution Using Physic Seed Hull (Jatropha curcas L.). Malaysia: Universiti Teknologi Petronas, 2010.
36. Sitko R, Zawisza B, Malicka E. Modification of carbon nanotubes for preconcentration, separation and determination of trace-metal ions. *TrAC Trends Anal Chem*. 2012;37:22–31.
37. Langmuir I. The adsorption of gases on plane surfaces of glass, mica and platinum. *J Am Chem Soc*. 1918;40(9):1361–1403.
38. Alslaibi TM, Abustan I, Ahmad MA, Abu Foul A. Application of response surface methodology (RSM) for optimization of Cu^{2+}, Cd^{2+}, Ni^{2+}, Pb^{2+}, Fe2+, and Zn^{2+} removal from aqueous solution using microwaved olive stone activated carbon. *J Chem Technol Biotechnol*. In press. DOI: 10.1002/jctb.4073.
39. Alslaibi TM, Abustan I, Ahmad MA, Abu Foul A. Preparation of activated carbon from olive stone waste: optimization study on the removal of Cu^{2+}, Cd^{2+}, Ni^{2+}, Pb^{2+}, Fe^{2+} and Zn^{2+} from aqueous solution using response surface methodology. *J Dispersion Sci Technol*. In press. DOI: 10.1080/01932691.2013.809506.
40. Li Q, Zhai J, Zhang W, Wang M, Zhou J. Kinetic studies of adsorption of Pb (II), Cr (III) and Cu (II) from aqueous solution by sawdust and modified peanut husk. *J Hazard Mater*. 2007;141(1):163–167.
41. Xie R, Jiang W, Wang L, Peng J, Chen Y. Effect of pyrolusite loading on sewage sludge based activated carbon in Cu(II), Pb(II), and Cd(II) adsorption. *Environ Prog Sustainable Energy*. 2012.
42. Brown P, Atly Jefcoat I, Parrish D, Gill S, Graham E. Evaluation of the adsorptive capacity of peanut hull pellets for heavy metals in solution. *Adv Environ Res*. 2000;4(1):19–29.
43. Spinti M, Zhuang H, Trujillo EM. Evaluation of immobilized biomass beads for removing heavy metals from wastewaters. *Water Environ Res*. 1995;67(6):943–952.
44. Tuzen M, Saygi KO, Soylak M. Solid phase extraction of heavy metal ions in environmental samples on multiwalled carbon nanotubes. *J Hazard Materials*. 2008;152(2):632–639.
45. Reddad Z, Gerente C, Andres Y, Le Cloirec P. Adsorption of several metal ions onto a low-cost biosorbent: kinetic and equilibrium studies. *Environ Sci Technol*. 2002;36(9):2067–2073.
46. Lim J, Kang H-M, Kim L-H, Ko S-O. Removal of heavy metals by sawdust adsorption: equilibrium and kinetic studies. *Environ Eng Res*. 2008;13(2):79.
47. Qiu H, Lv L, Pan B, Zhang Q, Zhang W. Critical review in adsorption kinetic models. *J Zhejiang Univ-Sci A*. 2009;10(5):716–724.
48. Anirudhan T, Sreekumari S. Adsorptive removal of heavy metal ions from industrial effluents using activated carbon derived from waste coconut buttons. *J Environ Sci*. 2011;23(12):1989–1998.
49. Çalışkan E, Bermúdez J, Parra J, Menéndez J, Mahramanlıoğlu M, Ania C. Low temperature regeneration of activated carbons using microwaves: Revising conventional wisdom. *J Environ Manage*. 2012;102:134–140.
50. Bashir MJK. Removal of Colour, COD and NH_3-N from Semi-aerobic Landfill Leachate Using Anionic and Cationic Resin. Malaysia: Universiti Sians Malaysia, 2010.
51. Ania C, Parra J, Menendez J, Pis J. Microwave-assisted regeneration of activated carbons loaded with pharmaceuticals. *Water Res*. 2007; 41(15):3299–3306.
52. Alslaibi TM, Abustan I, Ahmad MA, Abu Foul A. Comparison of Activated Carbon Prepared from Olive Stones by Microwave and Conventional Heating for Iron (II), Lead (II), and Copper (II) Removal from Synthetic Wastewater. *Environ. Prog. Sustainable Energy*. In press. DOI: 10.1002/ep.11877.

Manuscript received May 10, 2013, and revision received Sept. 3, 2013.